Journal of the Taiwan Institute of Chemical Engineers 000 (2015) 1–12

Contents lists available at ScienceDirect

Journal of the Taiwan Institute of Chemical Engineers

journal homepage: www.elsevier.com/locate/jtice

Multi-objective optimization method using an improved NSGA-II algorithm for oil–gas production process

Tan Liu[a,*], Xianwen Gao[a,b], Lina Wang[a]

[a] School of Information Science & Engineering, Northeastern University, Shenyang 110819, China
[b] National Key Laboratory of Integrated Automation for Process Industries, Northeastern University, Shenyang 110819, China

ARTICLE INFO

Article history:
Received 3 November 2014
Revised 24 March 2015
Accepted 17 May 2015
Available online xxx

Keywords:
Oil–gas production process
Multi-objective optimization
NSGA-II
Hybrid chaotic map model
Substitution operation
I-NSGA-II

ABSTRACT

By analyzing the characteristics of oil–gas production process and the relationship between subsystems, a multi-objective optimization model is proposed with maximizing the overall oil production, and minimizing the overall water production and comprehensive energy consumption for per ton oil. And then the non-dominated sorting genetic algorithm-II (NSGA-II) is used to solve the mode1. In order to further improve the diversity and convergence of Pareto optimal solutions obtained by NSGA-II algorithm, an improved NSGA-II algorithm (I-NSGA-II) is proposed. The algorithm is based on the basic NSGA-II, and the main improvements are as follows: Firstly, a new hybrid chaotic mapping model is established for population initialization. Secondly, the gradient operator is introduced, and it combines with the crossover and mutation operator to compose the hybrid operator by which a new generation of population is produced. Lastly, substitution operation of chaotic population candidate is used to select the new population. Finally, the performances of the proposed algorithm are demonstrated in actual production process of an oil recovery operation area studies, the results verify the effectiveness of the model and the algorithm.

1. Introduction

As the oil is continuously exploited, the industry of oil production is generally faced with some challenges such as the relative decline of the formation energy, higher and higher comprehensive water cut, gradual decline of the ground gathering system load, inefficiency, and gradual increase of the cost for per ton oil. Because the energy consumption of oil–gas gathering system and the pumping system accounts for a very large proportion of the energy consumption in oil–gas production process, many scholars have put forward the optimization models of related system and the energy saving methods, such as the researches on the modeling and optimization methods for sucker-rod pumping system and optimization methods for oil–gas gathering and transferring system. These methods have made progress on alleviating energy consumption, reducing production cost, and improving the economic benefit.

For the modeling and optimization methods for sucker-rod pumping system, domestic and foreign scholars have done a lot of work. For instance, in order to address the problem of excessive water output of oil well, Rabiei et al. [1] present a novel modeling approach to predict the water output, and the model parameters are identified by using production data. The results show that the water output of oil well is diagnosed accurately and timely, and it provides the possibility for taking the remedial actions. Aiming at the daily gas-lift wells scheduling in petroleum fields, and considering with the nonlinearity of the reservoir behavior, the multiphase flow in wells and constraints of the surface facilities, a novel mixed integer non-linear programming (MINLP) model is present by Kosmidis et al. [2]. The model can determine the operational status of wells (open or closed), the well oil rates and the allocation of gas-to-gas lift wells, and it achieves the maximum daily profit. Based on the established model, Camponogara et al. [3] also developed an automation system for integrated operation of gas-lift platforms. In China, Zheng and Deng [4] set up an optimization model in which a given output is taken as a constraint and the minimum energy consumption taken as the objective. When the method is applied in oilfields, it can effectively cut down the energy consumption and greatly improve the efficiency of sucker-rod pumping system. When the technical equipment conditions are certain, an optimization model is set up by Dong et al. [5] to improve the efficiency of sucker-rod pumping system, in which the suction parameters of the sucker-rod pumping system are taken as decision variables and the highest system efficiency is taken as the objective. The pump efficiency of sucker-rod pumping system is also improved by Wu et al. [6] through optimizing some influential variables. Aiming at the deficiencies when the single well is taken as the research object, the overall optimization model of an oil production block is

* Corresponding author. Tel.: +8618842361062.
E-mail address: liutan_0822@126.com (T. Liu).

http://dx.doi.org/10.1016/j.jtice.2015.05.026
1876-1070/

established by Dong et al. [7], in which the minimum overall input power is taken as objective and the planned oil production is taken as a constraint. According to comparison of optimization results of single well with the optimization results of the integral oil production block, it shows the superiority of the integral optimization strategy. For the intermittent pumping oil wells production process, the mixed integer nonlinear programming model is set up by Lang and Tang [8], in which the minimum start-up cost and production operating cost are the objectives, and the turn on/off time and oil flow rates of oil wells are the decision variables. And the Lagrange relaxation based heuristic is developed to solve the model. The numerical results illustrate that the algorithm can find the optimal solution in a relatively short time compared with the commercial solver CPLEX.

There are also many scholars who have done some work on optimization methods for the oil–gas gathering and transferring system; in these methods, the minimum production operation cost or total energy cost of oil pipeline is taken as the objective function. For example, a multi-objective optimization model is established for oil–gas gathering and transferring process of ring type mixing hot water with single or double pipes [9], in which the minimum total heat consumption, electricity consumption and investment are the objective functions, and the pressure, temperature and diameter range of pipes are the constraints. Then, the direct sequential quadratic programming method is used to solve the model. The results show the effectiveness of the method for reducing the total heat consumption, electricity consumption and investment of the gathering and transferring process. He et al. [10] also establishes the optimization model of gathering and transportation for electrical heating about ramiform net, where the lowest investment and operating cost is the objective function. And an improved POWELL method is used for solving the model. Computational experiments show that the proposed optimization method can reduce the total investment and the heating cost of the gathering and transferring system. Besides, an optimization method for heavy oil pipeline heating transportation is present by Wu [11], which can reduce the energy consumption significantly. Abbasi and Garousi [12] develop an efficient mixed-integer linear formulation for finding the optimal pump operation schedule, in the formulation, the lowest-cost energy consumption is the objective under some mandatory operational and physical constraints. It is applied in a Western Canadian oil pipeline, and GAMS's MILP solver (CPLEX 11.0) is used for solving the model, the results verification of the method is effective. For the natural gas pipeline, the optimization model is first established by Mahmoudimehr and Sanaye [13], in which the minimum fuel consumption of a natural gas compressor station is the objective. Then, genetic algorithm (GA) and the exhaustive search method (ES) is used to solve the model. Finally, the model and the optimization algorithm are validated by the results. In order to overcome the disadvantages of optimization model of natural gas pipeline transportation, Borraz-Sánchez and Haugland [14] incorporate the variations in pipeline flow capacities with gas specific gravity and compressibility in the optimization model, taking the maximum natural gas flow as the objective, and the flow, pressure, compressibility and specific gravity as decision variables. Then, a heuristic method is applied for solving the model, and the experimental results display a better performance of the method.

Although the above optimization researches for the single sucker-rod pumping system and the single oil–gas gathering and transportation system have made some progress, and obtained a certain effects in practice, they lack the overall consideration and usually take the single target as research objective. However, in the actual production process, we often need to consider the overall production process and pursue several objectives optimally instead of one single objective. Therefore, through analyzing the characteristics of the overall oil–gas production process and the relationship between subsystems, a nonlinear multi-objective optimization model is established. The paper is organized as follows. In Section 2, the oil–gas production process

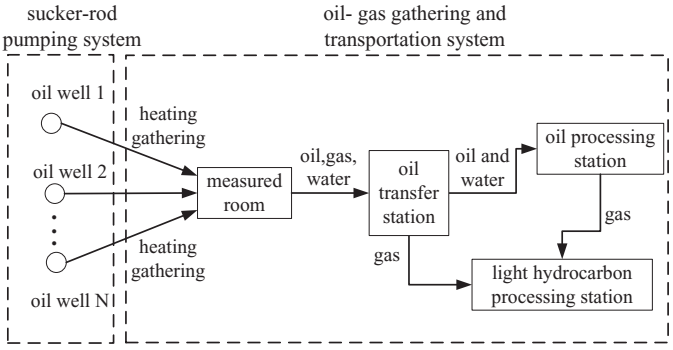

Fig. 1. Basic flowchart of oil–gas production process.

is described. In Section 3, a nonlinear multi-objective optimization model (NMOM) is established to maximize overall oil production of the block, minimizing overall water production and comprehensive energy consumption for per ton oil. Then, NSGA-II is used for solving the proposed optimization model, and in order to further improve the diversity and convergence of Pareto optimal solutions obtained by NSGA-II, an improved NSGA-II algorithm (I-NSGA-II) is proposed in Section 4. In Section 5, the performances of the proposed method are demonstrated in actual production process of an oil recovery operation area studies. Finally, conclusion is given in Section 6.

2. Description of oil–gas production process

In this paper, a whole block in an oil recovery operating area is taken as study object, and the flowchart of the oil–gas production process is shown in Fig. 1.

From Fig. 1, it is seen that oil–gas production process mainly includes the sucker-rod pumping system and oil–gas gathering and transportation system. The basic flow is as follows: the oil, gas and water mixture produced from oil wells is sent to the measured room for measuring after being heated by the wellhead heating furnace. Then, the mixed liquid is transported to the transfer station for the separation of gas and liquid. The separated natural gas is transported to the light hydrocarbon station through gas transmission pipeline for recycling, and the separated oil–water mixture is transported to the processing station through oil pipeline for crude oil dewatering and stabilizing. Finally, the dehydrated crude oil is put in storage or transmission. In the entire oil–gas production process, comprehensive energy consumption mainly refers to power consumption in the sucker-rod pumping system (electricity consumption), heat consumption (natural gas consumption) and power consumption (electricity consumption) in the gathering system.

The main pursue of oil production in oil industry is to realize energy saving and reduce the overall water output with the stable oil production or increased oil production. Thus, there are three production indices needed to be considered in the oil production, they are: overall oil production, overall water production and comprehensive energy consumption for per ton oil, respectively. Oil production is the production rate of oil after a series of processing, such as oil–gas separation, oil–water separation and oil dehydration. Usually, higher the oil production, higher the effective power is when input power is constant, therefore, higher the equipment utilization required. Comprehensive energy consumption for per ton oil is a measure of standard for energy consumption in oil production process, and it is equal to the overall comprehensive energy consumption divided by the overall oil production. Obviously, more the overall oil production and lower the overall energy consumption, lower is the comprehensive energy consumption for per ton oil.

Ideally, the three indices are expected to be the best simultaneously. However, it is very difficult, if not possible, to get such utopian

Please cite this article as: T. Liu et al., Multi-objective optimization method using an improved NSGA-II algorithm for oil-gas production process, Journal of the Taiwan Institute of Chemical Engineers (2015), http://dx.doi.org/10.1016/j.jtice.2015.05.026

result that all the indices are the best because there exist several mutual conflicts among them. For example, when one oil well reaches a certain output, continuing to increase in oil production will increase the power input in pumping system rapidly, and the transportation energy consumption in oil–gas gathering and transportation system is increased. Ultimately, higher oil production will lead to higher energy consumption in the entire system. Additionally, when water cut is certain or varies in a certain range, the increment of oil production will lead to the increment of the overall water production. Therefore, inappropriate assignment of these production indices may lead to the problem of poor product quality, and it is difficult to guarantee the continuity and stability of the production, even affect the economic benefit of oil industry.

In addition, the oil production is an integral process which consists of many wells, and the wells have impact on each other, so each well in the optimal state does not mean that the entire oil production block is in the optimal state. When the optimal operating conditions for a single well are determined, the status of the well most likely affect the production of other wells, thus, it may make the whole production system to deviate from the optimum working condition. In order to solve the problem, it is necessary to take the overall oil production process into consideration.

3. Multi-objective optimization model for oil–gas production process

3.1. Decision variables

Based on the basic flow of oil–gas production process and referring to the related literatures [5,9,11,12,15], the corresponding decision variables of each subsystem are selected by analyzing the entire production process. The stroke and the stroke times of each rod-pumped well in the block are selected as the decision variables of the sucker-rod pumping system. The heating temperature of wellhead heating furnace and pump head are selected as decision variables of the oil–gas gathering and transferring system. Therefore, the operating variables which play a key role in the optimization of oil–gas production process are selected as decision variables as follows.

$$\boldsymbol{X} = \{\boldsymbol{S}, \boldsymbol{n}, \boldsymbol{T}_w, \boldsymbol{H}\} \tag{1}$$

where $\boldsymbol{S} = [S_1, S_2, ..., S_J]^T$ and $\boldsymbol{n} = [n_1, n_2, ..., n_J]^T$ represent stroke and stroke times vectors, respectively. S_j and n_j are the stroke and the stroke times of the jth rod-pumped well, respectively. $\boldsymbol{T}_w = [T_{w1}, T_{w2}, ..., T_{wJ}]^T$ is the heating temperature vector of wellhead heating furnaces, and $\boldsymbol{H} = [H_1, H_2, ..., H_J]^T$ is the pump head vector.

3.2. The objective function

3.2.1. The model of maximizing overall oil production

Maximizing overall oil production of sucker-rod pumping system in the block is to make the whole oil production in the block platform largest by distributing the output of each oil well reasonably under a certain constraints, that is:

$$\max\ Q_0(\boldsymbol{X}) = \sum_{j=1}^{J} Q_j(1 - n_{wj}) \tag{2}$$

According to the equation $Q_j = 1440\pi D_j S_j n_j \alpha_j/4$, we can obtain

$$\max Q_0(\boldsymbol{X}) = \sum_{j=1}^{J} \frac{1440\pi D_j S_j n_j \alpha_j}{4}(1 - n_{wj}) \tag{3}$$

where $Q_0(\boldsymbol{X})$ is the overall oil production of the block platform, Q_j is the fluid production of the jth rod-pumped well, D_j, S_j, n_j and α_j are pump diameter, stroke, stroke times and pump efficiency of the corresponding oil well, respectively. n_{wj} is the water cut, and J is the number of rod-pumped wells. When the reservoir characteristics, crude oil physical property and suction parameters $(S, n, D, L, \{d_i, L_i\}_{i=1,2,...,I})$ are certain, the pump efficiency α is only the function of the submergence pressure p_s [5]. Then, basing on the oil well production capacity cooperative equation and the relationship between the bottom hole flowing pressure and the submergence pressure, Eq. (4) is formulated as follows:

$$\begin{cases} Q_{\max}\{1 - 0.2(\frac{p_{jf}}{p_{jr}}) - 0.8(\frac{p_{jf}}{p_{jr}})^2\} = 1440\frac{\pi}{4}D_j^2 S_j n_j \alpha_j \\ p_{jf} = p_{js} + (L_Z - L_j)\rho_{mj} g \end{cases} \tag{4}$$

where the previous equation is the cooperative equation of oil well production capacity, it means that the flow rate from the reservoir into the wellbore is equal to the actual production flow rate of oil well when the system is under the steady-state, p_{jf}, p_{jr} and p_{js} represent the flowing pressure, the static pressure and the submergence pressure of the jth rod-pumped well, respectively. L_Z is the central reservoir depth, L_j is downhole pump depth, and ρ_{mj} is oil–water mixture density. When reservoir characteristics and crude oil physical property are certain, p_{jf} and p_{js} are calculated under different suction parameters by Eq. (4), and then Q_j is obtained. Thus, it is considered that Q_j is the function of S_j and n_j when reservoir characteristics, crude oil physical property and $D, L, \{d_i, L_i\}_{i=1,2,...,I}$ are certain.

3.2.2. The model of minimizing overall water production

The formulation of minimizing overall water production in a block is as follows:

$$\min\ Q_w(\boldsymbol{X}) = \sum_{j=1}^{J} Q_j n_{wj} = \sum_{j=1}^{J} \frac{1440\pi D_j S_j n_j \alpha_j}{4} n_{wj} \tag{5}$$

Particularly, for water coning wells, the water production varies drastically with oil production, and they satisfy the following relationship [2].

$$\min\ Q_w(\boldsymbol{X}) = \sum_{j=1}^{J} f_0(Q_{0j}) \tag{6}$$

where Q_{0j} is oil production of the jth rod-pumped well, through analyzing the formulation of oil production and Eqs. (5) and (6), it is easy to see that $Q_w(\boldsymbol{X})$ is also the function of S_j and n_j when other parameters are constant.

3.2.3. The model of minimizing comprehensive energy consumption for per ton oil

The model of minimizing comprehensive energy consumption for per ton oil is as follows:

$$\min y(\boldsymbol{X}) = [Q_g Q_{DW} + (W_1 + W_2)R]/R_1 \tag{7}$$

where $W_1 = \sum_{j=1}^{J} W_{1j}/Q_0(\boldsymbol{X})$ represents the power consumption for per ton oil in sucker-rod pumping system, $W_2 = Q_p t/(\eta_p R Q_0(\boldsymbol{X}))$ and $Q_g = Q_T t/(\eta_T Q_{DW} Q_0(\boldsymbol{X}))$ represent power consumption and heat consumption (natural gas consumption) for per ton oil in oil–gas gathering and transportation system, respectively. $W_{1j} = P_j t$ is the power consumption of the jth rod-pumped well, P_j is the input power of system, t is the running time of oil well for 1 day, when equipment type and the management status are certain, P_j is the function of suction parameters [7], Q_T and Q_p are the total heat loss and the pressure loss of oil–gas gathering pipelines, respectively, and they can be calculated by Eq. (8) [9,12], η_T and η_p are efficiency of the related equipment, Q_{DW}, R and R_1 represent the low calorific value of the fuel, electrical energy conversion coefficient and equivalent to the heat value of per kilogram standard coal, respectively.

$$\begin{cases} Q_p = \sum_{i=1}^{N-1}\sum_{l=1}^{P} Q_{pi}^l = \sum_{i=1}^{N-1}\sum_{j=1}^{P} Q_i^l(p_i^l - p_{mi}^l) \\ Q_T = \sum_{i=1}^{N-1}\sum_{l=1}^{P} Q_{Ti}^l = \sum_{i=1}^{N-1}\sum_{l=1}^{P} C_i^l \rho_i^l Q_i^l (T_i^l - T_{mi}^l) \end{cases} \tag{8}$$

Please cite this article as: T. Liu et al., Multi-objective optimization method using an improved NSGA-II algorithm for oil-gas production process, Journal of the Taiwan Institute of Chemical Engineers (2015), http://dx.doi.org/10.1016/j.jtice.2015.05.026

where N is the level of pipe network, each well is in 1 level, measured room is in 2 level, and oil transfer station is in 3 level, P is the number of nodes for each level, Q_{pi}^l and Q_{Ti}^l are the pressure loss and heat loss of the lth pipeline in the ith level, respectively, Q_i^l is the volume flow rate of mixture in the corresponding pipeline, ρ_i^l is the mixture density, C_i^l is specific heat in the pipeline, $T_i^l - T_{mi}^l$ and $p_i^l - p_{mi}^l$ are the temperature drop and the pressure drop, respectively. The temperature drop is calculated as follows:

$$T_{mi}^l = (T_i^l - T_0)\mathrm{e}^{-K_1\pi d_i^l l_i^l/(C_i^l G_i^l)} + T_0 \tag{9}$$

where T_i^l and T_{mi}^l represent the inlet temperature and the outlet temperature of the lth pipeline in the ith level, G_i^l is mass flow rate of mixture in the corresponding pipeline, d_i^l and l_i^l are the diameter and length of the pipeline, T_0 is the ambient temperature of the pipeline, and K_1 is the heat transfer coefficient.

For oil pipeline, different Reynolds number (R_e) will lead to different flow state. For example, a low R_e indicates smooth or laminar flow. Otherwise, a high R_e indicates mixed or turbulent flow [9,16].

(1) when $R_e \le 2000$, the flow in oil gathering pipeline is laminar and the pressure drop is given in Eq. (10):

$$(p_i^l)^2 - (p_{mi}^l)^2 = 23,387\mu_i^l\eta_i^l T_{ai}^l G_i^l l_i^l/[d_g(d_i^l)^4] \tag{10}$$

(2) when $3000 \le R_e \le R_1$, the mixture is in turbulent smooth region and the pressure drop is given in Eq. (11):

$$\left(p_i^l\right)^2 - \left(p_{mi}^l\right)^2 = \frac{138.6\left(\mu_i^l\right)^{0.25}\eta_i^l\left(\eta_i^l+1\right)^{0.75}Z_s T_{ai}^l\left(G_i^l\right)^{1.75}l_i^l}{d_g\left(d_i^l\right)^{4.75}} \tag{11}$$

(3) when $R_1 \le R_e \le R_2$, the mixture is in turbulent mixed friction region and the pressure drop is as follows:

$$\left(p_i^l\right)^2 - \left(p_{mi}^l\right)^2 = \frac{48.33\left(\mu_i^l\right)^{0.128}\eta_i^l\left(\eta_i^l+1\right)^{0.877}Z_s T_{ai}^l\left(G_i^l\right)^{1.78}l_i^l}{d_g\left(d_i^l\right)^{4.877}} \tag{12}$$

(4) when $R_2 \le R_e$, the mixture is in turbulent rough region and the pressure drop is calculated in Eq. (13)

$$\left(p_i^l\right)^2 - \left(p_{mi}^l\right)^2 = \frac{465.27\lambda_i^l\eta_i^l\left(\eta_i^l+1\right)Z_s T_{ai}^l\left(G_i^l\right)^2 l_i^l}{d_g\left(d_i^l\right)^5} \tag{13}$$

where p_i^l and p_{mi}^l represent the inlet pressure and the outlet pressure of the lth pipeline in the ith level, respectively. μ_i^l is the kinematic viscosity of mixture in the corresponding pipeline, $\eta_i^l$is the air/liquid mass flow ratio, Z_s is the gas compressive coefficient, T_{ai}^l is the average temperature of mixture, d_g is the relative air density, λ_i^l is the friction factor, R_1 and R_2 are the parameters related to material and diameter of the corresponding pipeline, respectively.

For natural gas pipeline, the pressure drop can be calculated by Eq. (14).

$$p_i^l - p_{mi}^l = 0.4104\left(G_i^l\right)^2 d_g Z_s T_{ai}^l l_i^l/\left(d_i^l\right)^{5.33} \tag{14}$$

Through the above description, it is seen that the energy consumption of oil and gas pipelines is related to wellhead heating temperature, pump head, pipe diameter, fluid production of wells, water cut, *etc.*

3.3. Constraints

With the overall consideration, the constraints satisfy the following equations.

$$\begin{cases} \boldsymbol{S}_{\min} \le \boldsymbol{S} \le \boldsymbol{S}_{\max} \\ \boldsymbol{n}_{\min} \le \boldsymbol{n} \le \boldsymbol{n}_{\max} \\ \boldsymbol{T}_{w\min} \le \boldsymbol{T}_w \le \boldsymbol{T}_{w\max} \\ \boldsymbol{H}_{\min} \le \boldsymbol{H} \le \boldsymbol{H}_{\max} \\ Q_{\min} \le Q_0(\boldsymbol{X}) \\ T_l \ge [T_{\text{oil}}] = T_{\text{sol}} + (3 \sim 5), \quad \forall l \in P \\ T_{ol} \le T_{o\max}, \quad \forall l \in P \\ p_{qj} \le [p_o], \quad \forall j \in J \\ p_{zl} \ge [p_1], \quad \forall l \in P \end{cases} \tag{15}$$

In formula (15), the 1st inequality and the 2nd inequality are the stroke and stroke times constraints of rod-pumped wells, the 3rd inequality and the 4th inequality are the wellhead heating temperature and the pump head constraints, the 5th inequality is the overall oil production constraint. In these inequalities, the variables with subscript min and max represent the lower and upper limits of the corresponding variables, respectively. The 6th inequality is the temperature constraint where T_l is the temperature of the pipeline into oil transfer station, T_{sol} is the freezing point of oil. In order to keep the safety operation of oil gathering pipeline, the constraint of oil temperature out of oil transfer station represented by the 7th inequality needs to be considered, and $T_{o\max}$ is maximum allowable value of T_o. The 8th inequality is the wellhead back pressure constraint, and $[p_o]$ is the upper limit of the wellhead back pressure. The 9th inequality is the pressure constraint of oil pipeline into station, and $[p_1]$ is the minimum allowable value of pressure.

Basing on the above description, the variables in formula (1) are taken as the decision variables, formulas (3), (5), (6), and (7) are taken as the objective functions, and formula (15) is taken as constraint, then the multi-objective optimization model for oil–gas production process is obtained.

4. Multi-objective optimization for oil–gas production process based on improved NSGA-II algorithm

Solving the multi-objective optimization model for oil–gas production process belongs to a nonlinear multi-objective optimization problem with large constraints, decision variables including continuous variables and discrete variables and positive lower and upper bounded in practical production, as the development of population-based optimization techniques, the modern population-based algorithms have shown very promising performance. In addition, for solving multi-objective optimization problem, many traditional optimization methods are to convert multi-objective optimization problem into a single objective optimization problem by some methods and then the mature optimization algorithm such as SQP, or even global optimization methods are used to solve the optimization model, or to convert part of optimization objectives into the constraints for model optimization [17]. These traditional methods can ensure that every point gained usually has higher quality, but only produce one solution for each calculation and cannot guarantee Pareto optimality in the optimization process. To map the whole Pareto optimal frontier, the optimization procedure often should be repeated many times, which is a time-consuming process [18]. Evolutionary algorithms have been recognized to be well suited to multi-objective optimization, for example, one of the most efficient and commonly used versions of multi-objective GA (NSGA-II) can handle large and complex constraints by natural-inspired operators, and the NSGA-II algorithm has low computational complexity and good convergence by applying effective elite strategy than the previous

Please cite this article as: T. Liu et al., Multi-objective optimization method using an improved NSGA-II algorithm for oil-gas production process, Journal of the Taiwan Institute of Chemical Engineers (2015), http://dx.doi.org/10.1016/j.jtice.2015.05.026

evolutionary algorithms [15]; it has been successfully applied in solving many complex engineering optimization problems and achieved remarkable results [19–26]. First of all, NSGA-II is selected to solve the multi-objective optimization model for oil–gas production process, and then, in order to further improve the diversity and convergence of Pareto optimal solutions obtained by NSGA-II algorithm when solving the complicated and constrained optimization problems, an improved NSGA-II algorithm (I-NSGA-II) is proposed in this paper.

4.1. Analysis of standard NSGA-II algorithm

NSGA-II is the more representative algorithm in multi-objective optimization algorithms, which is first proposed by Deb et al. [27] based on the Non-dominated Sorting Genetic Algorithm (NSGA) [28], and it has many advantages than NSGA algorithm; the main features of NSGA-II algorithm are as follows: (1) using a fast non-dominated sorting to reduce the computational complexity, (2) introducing elitist strategy to expand the sample space and improve the accuracy of optimization results, (3) By defining the crowding distance, effectively overcome the need of NSGA to specify a special sharing parameter.

In order to improve the performance of NSGA-II algorithm, many scholars have put forward some improved algorithms. For example, in order to increase the diversity of population, the method to delete more repeated individuals generated by the tournament selection is proposed by Nojima et al. [29], and in order to improve the convergence of the algorithm, the gradient-based stochastic search methods are proposed by Shukla [30] and Brown and Smith [31], in which the new population is created by the variation of the gradient-based operator instead of the crossover operator or the mutation operator. The algorithm is suitable for the problems whose objective function gradient information is difficult to be directly calculated [32]. Although the above methods have made certain achievements, they only can improve a single performance of algorithm and have some deficiencies, for example, in the gradient-based stochastic search method, the difference between a point and its adjacent each local point is used to estimate the gradient information and the approximate Jacobi matrix of the point; this will increase the computation time and make the solved problem easy to fall into local optimum.

According to the above description, some inspirations are obtained, and the following improvement strategies are proposed in this paper.

4.2. Key operations for improved NSGA-II (I-NSGA-II) algorithm

In order to further improve the diversity and search capabilities of the non-dominated solutions obtained by NSGA-II algorithm, an improved strategy of NSGA-II algorithm is put forward in this paper. Firstly, a new hybrid chaotic mapping model is established to initialize population for keeping the diversity of the initial population. Secondly, the gradient operator is introduced, which combines with crossover and mutation operator to compose the hybrid operator, and then the hybrid operator is used to produce the new population for improving the search ability of algorithm. Finally, when choosing a new generation of population, chaotic population candidate is applied to implement substitution operation according to certain conditions for keeping the diversity and the uniformity of the new generation of population. With the improved operations, I-NSGA-II algorithm not only guarantees the uniformity and the diversity of the initial population and non-dominated solutions, but also improves the convergence of the algorithm to a large extent.

4.2.1. New hybrid chaotic mapping model

The most commonly used chaotic map model is the logistic map model [33], it is expressed as follows:

$$u_{k+1} = \mu u_k(1-u_k), \quad 0 \le u_k \le 1 \tag{16}$$

Although the logistic map model can usually satisfy the requirements of the population initialization, the points generated by the model appear at the region [0, 1] with a far less probability than at both boundaries of the interval, which makes the uniformity of these points bad. In contrast with the logistic map model, the tent map model [34] can generate points with a uniform distribution in the whole range of [0, 1], however, it always tends to 0 after several iterations. So it can be seen that the single logistic map model or the single tent map model has some defects in population initialization. Therefore, a method of combining two mapping models [35] is used in this paper to form a new hybrid chaotic mapping model, it is the tent map combined with the logistic map, and the fixed points of the tent map model can be eliminated by the slight disturbance of the logistic map model without changing the amplitude of the tent map model. The new hybrid chaotic map model is:

$$\begin{aligned} u_{k+1} &= \mu u_k(1-u_k), \quad 0 \le u_k \le 1 \\ r_{k+1} &= \begin{cases} \dfrac{1}{1.001}(2r_k + 0.001u_k), & 0 \le r_k \le 0.5 \\ \dfrac{1}{1.001}(2(1-r_k) + 0.001u_k), & 0.5 < r_k \le 1 \end{cases} \end{aligned} \tag{17}$$

In formula (17), μ is control parameter, when the initial values of r_k and u_k are selected as n random numbers between 0 and 1, that is: $0 \le r_{j1}^0 \le 1$, $0 \le u_{j1}^0 \le 1$, $j = 1, 2..., n$, we can obtain $r_{j,i+1}^0$ as follows:

$$\begin{aligned} u_{j,i+1}^0 &= \mu u_{ji}^0(1-u_{ji}^0), \quad 0 \le u_{ji}^0 \le 1 \\ r_{j,i+1}^0 &= \begin{cases} \dfrac{1}{1.001}(2r_{ji}^0 + 0.001u_{ji}^0), & 0 \le r_{ji}^0 \le 0.5 \\ \dfrac{1}{1.001}(2(1-r_{ji}^0) + 0.001u_{ji}^0), & 0.5 < r_{ji}^0 \le 1 \end{cases} \end{aligned} \tag{18}$$

Then, the produced chaotic variables are mapped to the decision variables, and the jth decision variable x_{ji}^0 of ith initialized individual X_i^0 is obtained as follows:

$$\begin{aligned} &x_{ji}^0 = x_{j\ \min} + (x_{j\ \max} - x_{j\ \min})r_{ji}^0 \\ &j = 1, 2, \ldots, n, \quad i = 1, 2, \ldots, N_P \end{aligned} \tag{19}$$

where $x_{j\min}$ and $x_{j\max}$ is the minimum and maximum value of the jth decision variables, n is the dimension number of decision variable vector, and N_P is the population size. The pseudocode for initializing population by the new hybrid chaotic mapping model is shown in Fig. 2.

From Fig. 2, it is seen that the computational complexity for initializing population by the new hybrid chaotic mapping model is $O(nN_P)$.

4.2.2. The gradient-based hybrid operator

It is well known that the negative gradient direction is the fastest direction to reduce the value of objective function, so in order to reduce the invalid trial times of crossover and mutation, the gradient operator is introduced in NSGA-II algorithm and combined with crossover and mutation operator to make up hybrid operator [36], then the hybrid operator is used to produce a new generation of population, its expression is shown as follows:

$$\omega_1 \text{operator}_C \oplus \omega_2 \text{operator}_M \oplus \omega_3 \text{operator}_G \tag{20}$$

where $\omega_i \ge 0,\ i = 1, 2, 3$ represents the probability for each operator execution separately, formula (20) means that the "child" solutions are created by the crossover operator with the probability ω_1, the mutation operator with the probability ω_2 and the gradient-based operator with the probability ω_3, operator_G represents the gradient

```
Set n : dimension number of decision variable vector
μ : control parameters
N_p : Population size
for i = 1 : N_p
{ for j = 1 : n
  { r_j1^0 = random (1)
    u_j1^0 = random (1)
    u_j,i+1^0 = μ u_ji^0 (1 − u_ji^0)
    If r_ji^0 >= 0 and r_ji^0 <= 0.5
    { r_j,i+1^0 = 1/1.001 (2 r_ji^0 + 0.001 u_ji^0)
      x_ji^0 = x_j min + (x_j max − x_j min) r_ji^0
    }
    elseif r_ji^0 > 0.5 and r_ji^0 <= 1
    {
      r_j,i+1^0 = 1/1.001 (2(1 − r_ji^0) + 0.001 u_ji^0)
      x_ji^0 = x_j min + (x_j max − x_j min) r_ji^0
    }
  }
}
```

Fig. 2. Pseudocode for initializing population by the new hybrid chaotic mapping model.

operator, and it is defined as follows:

$$\nabla_{m\times n} f(\boldsymbol{x}) = \begin{bmatrix} (\nabla f_1)^T \\ (\nabla f_2)^T \\ \cdot \\ \cdot \\ \cdot \\ (\nabla f_m)^T \end{bmatrix} = \begin{bmatrix} \frac{\partial f_1(\boldsymbol{x})}{\partial x_1} & \frac{\partial f_1(\boldsymbol{x})}{\partial x_2} & \cdots & \frac{\partial f_1(\boldsymbol{x})}{\partial x_n} \\ \frac{\partial f_2(\boldsymbol{x})}{\partial x_1} & \frac{\partial f_2(\boldsymbol{x})}{\partial x_2} & \cdots & \frac{\partial f_2(\boldsymbol{x})}{\partial x_n} \\ \cdot & \cdot & & \cdot \\ \cdot & \cdot & & \cdot \\ \cdot & \cdot & & \cdot \\ \frac{\partial f_m(\boldsymbol{x})}{\partial x_1} & \frac{\partial f_m(\boldsymbol{x})}{\partial x_2} & \cdots & \frac{\partial f_m(\boldsymbol{x})}{\partial x_n} \end{bmatrix} \tag{21}$$

where $f(\boldsymbol{x}) = [f_1(\boldsymbol{x}), f_2(\boldsymbol{x}), \cdots, f_m(\boldsymbol{x})]^T, \boldsymbol{x} \in R^n$ represents a multi-objective function and $f(\boldsymbol{x})$ is first-order continuous partial differential in the feasible region, recall further that the partial derivative $\partial f(\boldsymbol{x})/\partial x_i$ of f can be expressed as follows:

$$\frac{\partial f(\boldsymbol{x})}{\partial x_i} = \lim_{t\to 0}\left\{\frac{f(\ldots, x_i + t, \ldots) - f(\ldots, x_i, \ldots)}{t}\right\} \tag{22}$$

Then search direction can be obtained by the gradient operator:

$$e = \frac{d}{\|d\|} = -\sum_{i=1}^{m}\lambda_i \frac{\nabla f_i(x)}{\|\nabla f_i(x)\|} \Big/ \left\|\sum_{i=1}^{m}\lambda_i \frac{\nabla f_i(x)}{\|\nabla f_i(x)\|}\right\| \tag{23}$$

$$d = -\sum_{i=1}^{m}\lambda_i \frac{\nabla f_i(x)}{\|\nabla f_i(x)\|} \tag{24}$$

where $\lambda_i,\ i = 1, 2, \cdots, m$ is the random number between 0 and 1, the vector d is a convex cone of all the unit negative gradient vectors, and the search direction e is the normalized vector of d. The existence of the hybrid operator not only improves the chance of jumping out of the local optimum when the algorithm is in search, but also improves the search ability of the algorithm. The pseudocode for creating "children" by hybrid operator is shown in Fig. 3.

The computational cost of gradient-based operator mainly includes gradient estimation and the line search. As mentioned above,

```
Set N_p : Population size
t_0 : Initial step length
for G=1 to G_max //generation number
 { for i = 1 : N_p
   { if random (1) ≤ ω_1 //crossover step
     {
       x_i^{G+1} = child-Crossover
     }
   }
   for i = 1 : N_p
   { if random (1) ≤ ω_2 //mutation step
     {
       x_i^{G+1} = child-Mutation
     }
   }
   for i = 1 : N_p
   { if random (1) ≤ ω_3 //gradient-based operator
     {
       x_i^G = population(j)
       t_G = t_0 (G_max − G+1) / G_max //stepsize
       e = d/‖d‖ = −Σ_{j=1}^{m} λ_j ∇f_j(x_i^G)/‖∇f_j(x_i^G)‖ / ‖Σ_{j=1}^{m} λ_j ∇f_j(x_i^G)/‖∇f_j(x_i^G)‖‖
       x_i^{G+1} = x_i^G + t_G e
     }
   }
   newchild = x^{G+1}
 } //end for
```

Fig. 3. Pseudocode for creating "children" by hybrid operator.

the computational complexity for the line search is $O(mnN_P)$. For gradient estimation, if the formulation of objective functions is known, the gradient can be obtained directly and there are no additional evaluations to be needed. Therefore, the computational complexity for gradient-based operator is $O(mnN_P)$. When it is impossible to obtain the gradient of objective functions directly, the computational complexity for gradient estimation is $O(mnN_PF)$, and the overall computational complexity of gradient-based operator is also $O(mnN_PF)$. m and F are the number of objective functions and the complexity for a single gradient evaluation as given in formula (22), respectively.

4.2.3. Substitution operation of chaotic population candidate

In order to keep the diversity of obtained non-dominated solutions, in the evolution, when the measurement parameter of the population diversity λ^G is lower than $\lambda_{\min}$ and the population does not reach the optimal, the chaotic population candidate should replace the poor individuals according to a certain probability, which can guide the algorithm escape from local optima. When replacing, the higher Pareto rank in NSGA-II and the smaller crowding distance of the individuals, the higher probability is to be replaced. The probability can be calculated as follows:

$$P = i/N_p \tag{25}$$

where i is the sorting of individuals in the population, the higher Pareto rank in NSGA-II and the smaller crowding distance of the individuals, the more rearward sorting in population. $\lambda^G \in [0, 1]$ can be calculated by Eq. (26):

$$\lambda^G = \frac{1}{nN_P}\sum_{j=1}^{n}\frac{\sum_{i=1}^{N_P}\left|x_{ji}^G - x_j^G\right|}{x_{j\ \max} - x_{j\ \min}} \tag{26}$$

Set n: dimension number of decision variable vector
μ_1 : control parameters
N_p : Population size
$X^G = \{X_1^G, X_2^G, ..., X_{N_p}^G\}$: The G-th generation population
$N_{F_{1r}}^G$: Number of individuals with Pareto rank 1
for $G = 1$ to G_{max} //generation number
{ for $i = 1 : N_p$
{ for $j = 1 : n$
{
$r_{ji}^G = \mu_1 r_{ji}^{G-1}(1 - r_{ji}^{G-1})$
$x_{ji}^{'G} = x_{j\,min} + (x_{j\,max} - x_{j\,min}) r_{ji}^G$ //chaotic population candidate
}
}
$x_j^G = \sum_{i=1}^{N_p} x_{ji}^G / N_p$
$\lambda^G = \frac{1}{nN_p} \sum_{j=1}^{n} \frac{\sum_{i=1}^{N_p} \left| x_{ji}^G - x_j^G \right|}{x_{j\,max} - x_{j\,min}}$ //population diversity
for $i = 1 : N_p$
{ If $N_{F_{1r}} \neq N_p$ and $\lambda^G < \lambda_{min}$ and random $(1) < i / N_p$
{
$X_i^G = X_i^G$ // Substitution operation
}
}
} //end for
Pareto optimal solutions= $X^{G_{max}}$

Fig. 4. Pseudocode for substitution operation of chaotic population candidate.

$$x_j^G = \sum_{i=1}^{N_P} x_{ji}^G / N_P \tag{27}$$

Based on $r_{j,i+1}^0$, the jth component of ith individual of the chaotic population candidate x_{ji}^{G+1} is expressed as follows:

$$r_{ji}^{G+1} = \mu_1 r_{ji}^G (1 - r_{ji}^G) \tag{28}$$

$$x_{ji}^{G+1} = x_{j\,\min} + (x_{j\,\max} - x_{j\,\min}) r_{ji}^{G+1} \tag{29}$$

where $G = 0, 1, ..., G_{\max} - 1$ is evolutionary generation, and $G_{\max}$ is the maximum evolutionary generation. In this paper, the control parameter μ_1 is set to 3.6. The pseudocode for substitution operation is shown in Fig. 4.

From the above analysis, it is known that the computational complexity for substitution operation of chaotic population candidate is $O(nN_P)$.

In summary, if the gradient of objective function can be obtained directly, the overall computational complexity of the proposed algorithm is $O(nN_P) \cup O(mnN_P) \cup O(nN_P) \cup O(mN_P^2) = O(mnN_P + mN_P^2)$, otherwise, the overall computational complexity is $O(nN_P) \cup O(mnN_PF) \cup O(nN_P) \cup O(mN_P^2) = O(mnN_PF + mN_P^2)$, where $O(mN_P^2)$ is the computational complexity of NSGA-II algorithm [18].

4.3. The multi-objective optimization implementation for oil–gas production process based on I-NSGA-II algorithm

The design variables in the multi-objective optimization model for oil–gas production process both include discrete variables and continuous variables, using binary encoding for discrete variables $\boldsymbol{S}$ and real encoding for continuous variables $\boldsymbol{n}$, $\boldsymbol{T_w}$ and $\boldsymbol{H}$. The flow of the proposed I-NSGA-II algorithm for the multi-objective optimization of oil–gas production process is shown in Fig. 5.

5. Example analysis

5.1. Analysis of the algorithm performance

In order to prove that the convergence, the distribution diversity and the uniformity of Pareto optimal solutions obtained by improved algorithm is better than NSGA-II algorithm, hypervolume indicator I_H [37] and the uniformity metric Δ [33] are used to evaluate the algorithm performance.

The hypervolume indicator I_H is used to evaluate the approximation degree of the solution set to the real Pareto-optimal set, $I_H(A)$ of a solution set $A \subseteq X$ can be defined as the hypervolume of the space that is dominated by the set A and is bounded by a reference point $r = (r_1, ..., r_m) \in R^m$, it can be expressed as follows:

$$I_H(A) = \lambda\left(\bigcup_{a \in A} [f_1(a), r_1] \times ... \times [f_m(a), r_m] \right) \tag{30}$$

where $\lambda(S)$ is the Lebesgue measure of a set S and $[f_1(a), r_1] \times ... \times [f_m(a), r_m]$ is the m dimensional hypercuboid consisting of all points that are weakly dominated by the point α but not weakly dominated by the reference point. Greater the value of $I_H(A)$, better the convergence to the real Pareto-optimal front.

The diversity metric Δ means the extent of spread among the obtained non-dominated solutions, it is expressed as follows:

$$\Delta = \frac{d_f + d_l + \sum_{i=1}^{N_p - 1} \left| d_i - \bar{d} \right|}{d_f + d_l + (N_p - 1)\,\bar{d}} \tag{31}$$

where d_f and d_l represent the Euclidean distances between the extreme target vectors in the real Pareto-optimal front $\boldsymbol{P}_{\mathrm{F}}^*$ and the boundary target vectors in the obtained objective domain, d_i represents Euclidean distance between two adjacent target vectors in the obtained objective domain, $\bar{d}$ is the average value of all the distances d_i, $i = 1, 2, \cdots, (N_p - 1)$. Smaller the value of the diversity metric, the better the diversity of non-dominated solutions becomes.

5.2. Experimental results and analysis

I-NSGA-II algorithm is tested on several standard test problems including ZDT1, ZDT3 [38] and TNK [27], and in order to verify the superiority of proposed algorithm, I-NSGA-II algorithm is compared with original NSGA-II algorithms and some other improved algorithms, namely chaotic differential evolution for multi-objective optimization (CDEMO) [39] and gradient-based NSGA-II (G-NSGA-II) [36]. The related parameters of the algorithms are set as follows: the population size $N_P = 100$, maximum number of evaluations (Max.eval) are 20,000 and 90,000, respectively, distribution indexes for real encoding crossover operator and mutation operator of 20 and 20, the crossover operator probability ω_1 is set to 0.9, the mutation operator probability ω_2 is set to $1/n$ (n is the number of the decision variables), the control parameter of hybrid chaotic mapping model μ is set to 4, initial step length of the gradient operation $t_0 = 0.1$. Each algorithm is run 10 times on each problem instance. For one random run, the non-dominated solutions obtained by the algorithms are shown in Figs. 6–8, and the average hypervolume indicator I_H, the diversity metric Δ and their variances are listed in Tables 1–6.

From Figs. 6–8, it is seen that the points obtained by NSGA-II are mostly dominated by the points achieved by G-NSGA-II, CDEMO and I-NSGA-II with Max.eval = 20, 000, the non-dominated optimal objective domains obtained by CDEMO and I-NSGA-II are well close to

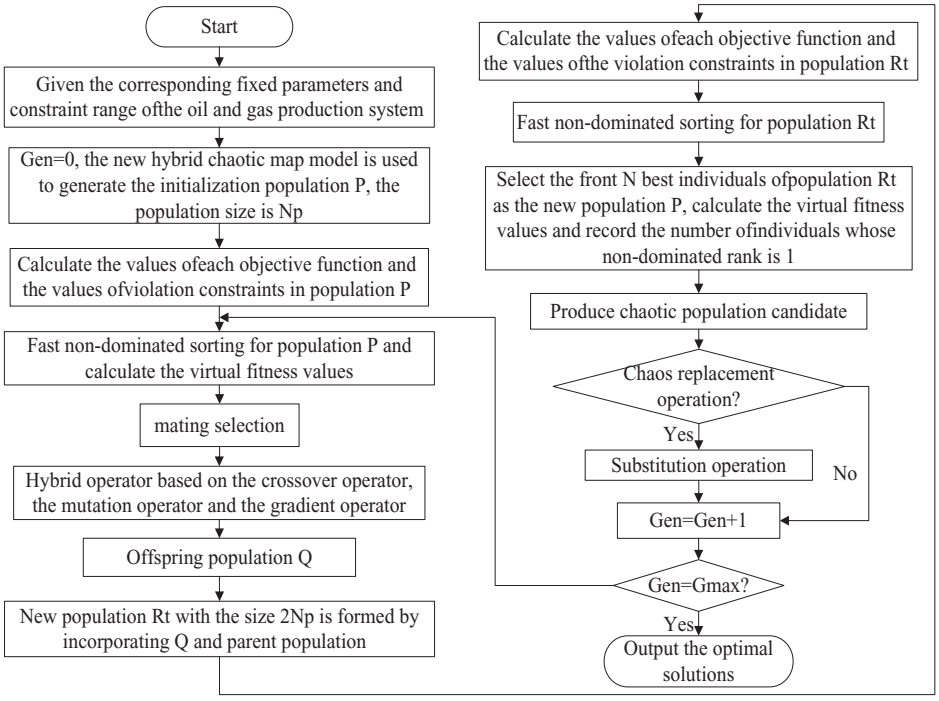

Fig. 5. Flow chart of multi-objective optimization for the oil–gas production process based on I-NSGA-II algorithm.

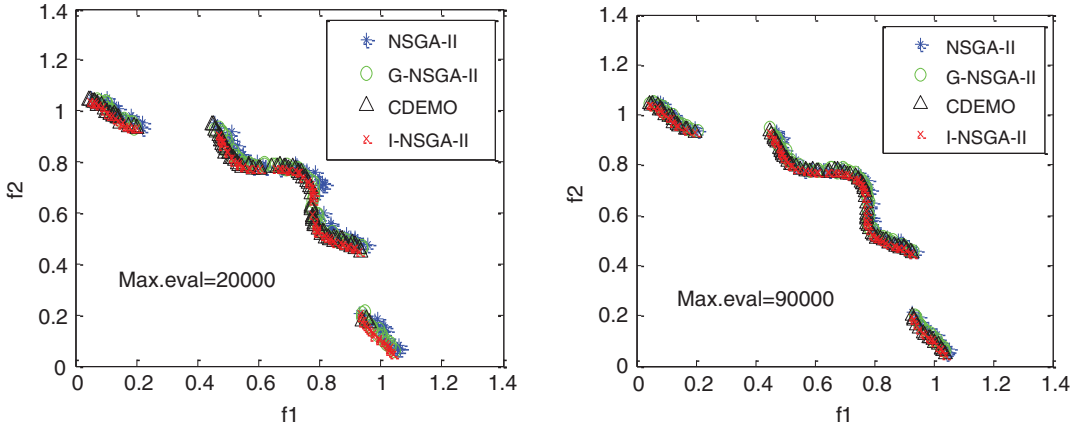

Fig. 6. Non-dominated solutions obtained by NSGA-II, G-NSGA-II, CDEMO and I-NSGA-II on problem TNK.

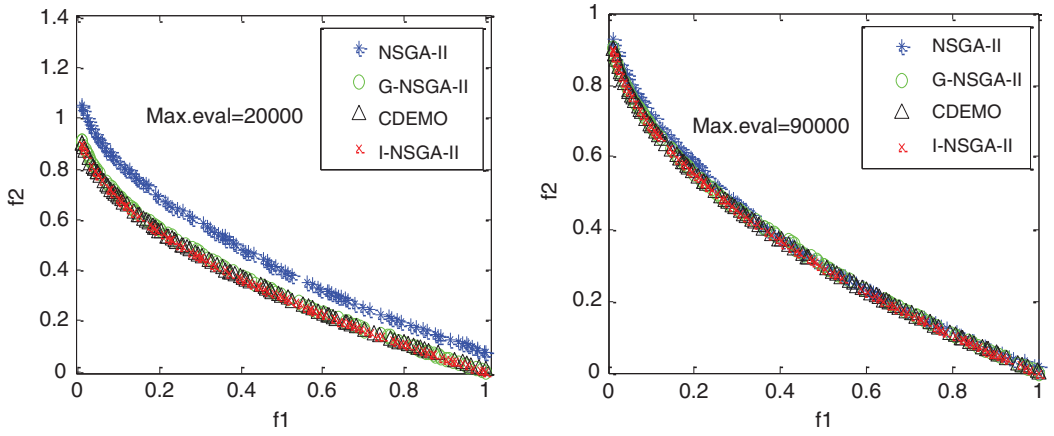

Fig. 7. Non-dominated solutions obtained by NSGA-II, G-NSGA-II, CDEMO and I-NSGA-II on problem ZDT1.

Please cite this article as: T. Liu et al., Multi-objective optimization method using an improved NSGA-II algorithm for oil-gas production process, Journal of the Taiwan Institute of Chemical Engineers (2015), http://dx.doi.org/10.1016/j.jtice.2015.05.026

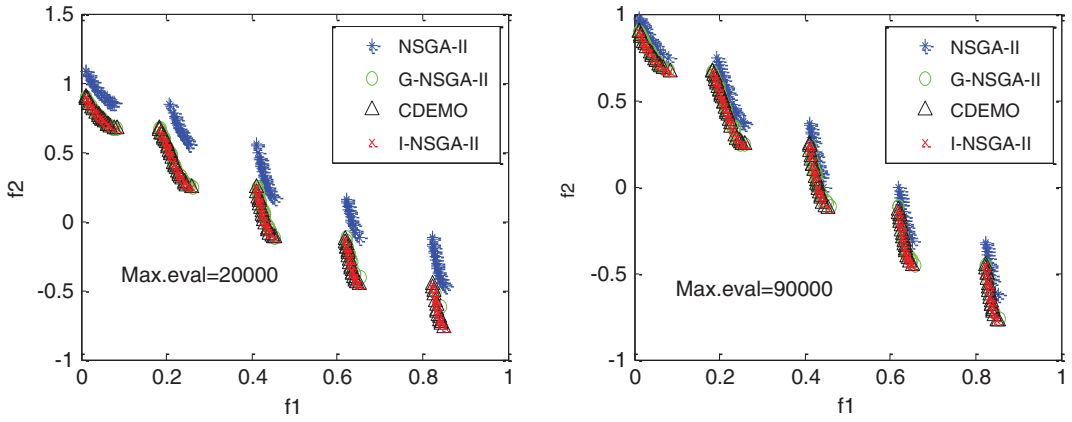

Fig. 8. Non-dominated solutions obtained by NSGA-II, G-NSGA-II, CDEMO and I-NSGA-II on problem ZDT3.

Table 1
Average value and variance of the convergence metric I_H on TNK.

Algorithm	Average I_H		Variance	
	Evaluations = 20,000	Evaluations = 90,000	Evaluations = 20,000	Evaluations = 90,000
(1) NSGA-II	0.53853	0.54025	3.49E-7	1.26E-7
(2) G-NSGA-II	0.54856	0.54979	2.51E-7	5.49E-8
(3) CDEMO	0.54769	0.54823	2.63E-7	5.36E-8
(4) I-NSGA-II	0.54892	0.54983	2.47E-7	4.89E-8

Table 2
Average value and variance of the diversity metric Δ on TNK.

Algorithm	Average Δ		Variance	
	Evaluations = 20,000	Evaluations = 90,000	Evaluations = 20,000	Evaluations = 90,000
(1) NSGA-II	0.848073	0.430354	0.009317	0.005175
(2) G-NSGA-II	0.560354	0.379423	0. 003169	0.002143
(3) CDEMO	0.395345	0.343237	0.003585	0.001849
(4) I-NSGA-II	0.363462	0.340231	0.001753	0. 000691

Table 3
Average value and variance of the convergence metric I_H on ZDT1.

Algorithm	Average I_H		Variance	
	Evaluations = 20,000	Evaluations = 90,000	Evaluations = 20,000	Evaluations = 90,000
(1) NSGA-II	0.81532	0.82569	0.005234	0.004965
(2) G-NSGA-II	0.82685	0.82686	0.000056	0. 000052
(3) CDEMO	0.82675	0.82683	0.000085	0. 000078
(4) I-NSGA-II	0.82692	0.82689	0. 000054	0. 000049

Table 4
Average value and variance of the diversity metric Δ on ZDT1.

Algorithm	Average Δ		Variance	
	Evaluations = 20,000	Evaluations = 90,000	Evaluations = 20,000	Evaluations = 90,000
(1) NSGA-II	0.41076	0.38291	0.001890	0.001753
(2) G-NSGA-II	0.35630	0.33811	0.001937	0.001589
(3) CDEMO	0.20417	0.172915	0.026850	0.024596
(4) I-NSGA-II	0.18534	0.15296	0.001481	0.001245

Table 5
Average value and variance of the convergence metric I_H on ZDT3.

Algorithm	Average I_H		Variance	
	Evaluations = 20,000	Evaluations = 90,000	Evaluations = 20,000	Evaluations = 90,000
(1) NSGA-II	0.69575	0.69779	0.008023	0. 007895
(2) G-NSGA-II	0.69783	0.69787	0.000062	0. 000059
(3) CDEMO	0.69785	0.69792	0.000078	0. 000075
(4) I-NSGA-II	0.69796	0.70295	0. 000060	0. 000056

Please cite this article as: T. Liu et al., Multi-objective optimization method using an improved NSGA-II algorithm for oil-gas production process, Journal of the Taiwan Institute of Chemical Engineers (2015), http://dx.doi.org/10.1016/j.jtice.2015.05.026

Table 6
Average value and variance of the diversity metric Δ on ZDT3.

Algorithm	Average Δ		Variance	
	Evaluations = 20,000	Evaluations = 90,000	Evaluations = 20,000	Evaluations = 90,000
(1) NSGA-II	0.75924	0.71103	0.019809	0.017956
(2) G-NSGA-II	0.64392	0.57634	0.003687	0. 003569
(3) CDEMO	0.26462	0.23478	0.024569	0. 023154
(4) I-NSGA-II	0.214270	0.19556	0. 001337	0. 001165

the real Pareto-optimal front and have a better uniform distribution along the real Pareto-optimal front with Max.eval = 90, 000. From the Tables 1– 6, it is seen that the performances of I-NSGA-II on the three test problems of TNK, ZDT1 and ZDT3 are better than NSGA-II and also slightly better than G-NSGA-II and CDEMO in terms of the coverage indicator I_H and the diversity metric Δ, and it further indicated that the non-dominated solutions obtained by I-NSGA-II have better convergence and uniformity for distribution along the real Pareto optimal set than other algorithms. In addition, the variance of I_H and Δ obtained by I-NSGA-II is smaller than other algorithms, which also indicated the proposed algorithm has better reliability.

5.3. Model solution and analysis

In order to verify the effectiveness of proposed optimization method, matlab programming is used to optimize design for oil–gas production process, and the production process with seven oil wells in an oil recovery operation area is taken for example, then, NSGA-II algorithm and I-NSGA-II algorithm are used to solve the established multi-objective optimization model, and the simulation results were compared.

The constraints are set as follows: the lower and upper limits of the jth rod pumped well stroke $s_{j\min} = 1$ and $s_{j\max} = 6$, the lower and upper limits of the jth rod pumped well stroke times are $n_{j\min} = 2$ and $n_{j\max} = 12$, the allowable temperature of crude oil getting into station $T_{\text{oil}} = 35^{\circ}$C, and the allowable temperature of crude oil out of station $T_{o\max} = 80^{\circ}$C, the pressure of oil pipeline getting into station is set to 0.2 MPa, maximum evolutionary generation of the optimization algorithm is $G_{\max} = 100$. Both NSGA-II algorithm and I-NSGA-II algorithm for solving the multi-objective optimization problem of oil–gas production process are run for 10 times, the optimization results of a random run are shown in Fig. 9, part of Pareto optimal solutions obtained by I-NSGA-II algorithm are listed in Table 7 and y represents comprehensive energy consumption for per ton oil.

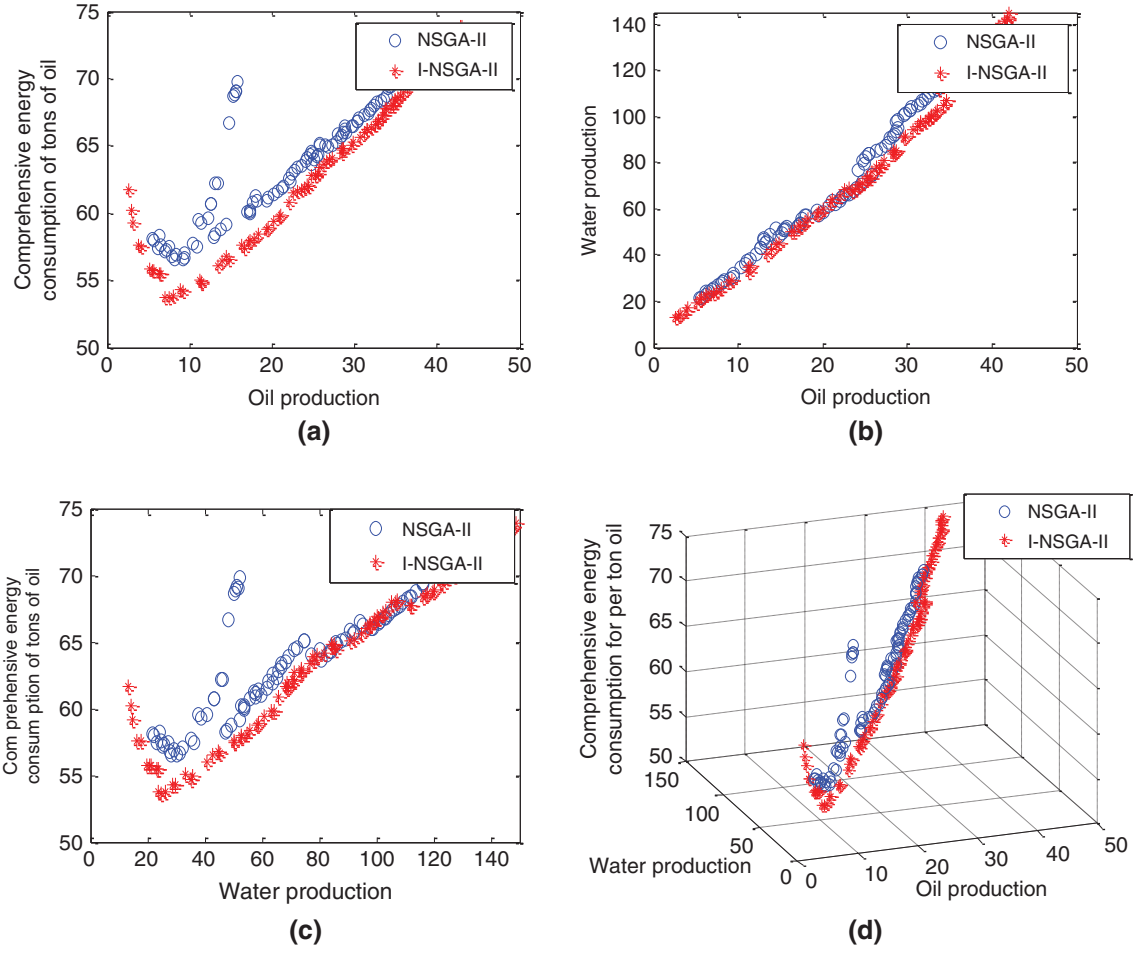

Fig. 9. Distribution chart of Pareto set obtained by NSGA-II, I-NSGA-II algorithm.

Table 7
Pareto optimal solutions obtained by I-NSGA-II algorithm.

Solution	Oil production/(t/d)	Water production/(t/d)	y/(kg/t)
1	42.9107	149.2196	73.8503
2	39.6509	134.8175	71.3352
3	33.4306	102.0396	67.2169
4	28.3915	83.7827	64.7920
5	17.8817	54.4883	58.1100
6	7.4548	24.1163	53.6675
7	5.7310	22.0692	55.6911
8	2.9351	13.9429	60.2143
9	2.5655	12.8420	61.7068

Table 8
Hypervolume indicator of NSGA-II algorithm and I-NSGA-II algorithm.

Numbers of running	Hypervolume indicator I_H	
	NSGA-II	I-NSGA-II
1	0.4817	0.4834
2	0.4634	0.4918
3	0.4930	0.4968
4	0.3962	0.4649
5	0.4823	0.5010
6	0.3742	0.4912
7	0.4577	0.5134
8	0.4634	0.4918
9	0.4903	0.5149
10	0.4795	0.4903
Variance	0.00164	0.00021

In Fig. 9, it can be seen that a set of Pareto optimal solutions are obtained by both algorithms, but the Pareto optimal solutions obtained by I-NSGA-II algorithm are superior to the solutions obtained by NSGA-II algorithm, and it can provide more feasible solutions for decision makers.

From Table 7, it is easy to see that solution 1, solution 9 and solution 6 are corresponding to the largest overall oil production, the least overall water production and comprehensive energy consumption for per ton oil in block platform, respectively. Other six solutions are relatively balanced. Thus, decision-making department can choose oil production scheme according to different objective requirements, *e.g.* at the initial stage of production, the main purpose of oil production in oil recovery enterprise is to maximize overall oil production with a certain range of energy consumption, and decision maker can give the production guide as solution 1 (42.9107 t/d, 149.2196 t/d, 73.8503 kg/t), at the middle or late stage, the main purpose of oil production is to minimize energy consumption with overall oil production in a certain range, decision maker can give the production guide as solution 6 (7.4548 t/d, 24.1163 t/d, 53.6675 kg/t). By solving the model, it can reduce overall energy consumption for per ton oil and improve overall oil production in a certain range. Ultimately, the economic benefit of enterprises can be improved.

Both NSGA-II algorithm and I-NSGA-II algorithm are used to solve the multi-objective optimization model of oil–gas production process for 10 times, and the corresponding hypervolume indicator I_H and deviation metrics Δ are listed in Tables 8 and 9, respectively.

From Tables 8 and 9, it can be seen that each hypervolume values (I_H) of the Pareto optimal solution set obtained by I-NSGA-II algorithm is greater than the corresponding hypervolume values of the Pareto optimal solution set obtained by NSGA-II algorithm, it further proves that the Pareto optimal objective domain obtained by the improved algorithm is more close to the real Pareto front. And the deviation metrics Δ of the Pareto optimal solution set obtained by I-NSGA-II algorithm is smaller than the corresponding deviation metrics obtained by NSGA-II algorithm, so it demonstrates the Pareto optimal solution set obtained by I-NSGA-II algorithm has a better uniformity. In addition, variances of I_H and Δ obtained by I-NSGA-II for 10 runs are 0.00021 and 0.09347, respectively. And they are smaller than the ones obtained by NSGA-II, which proves the reliability of proposed algorithm.

Table 9
Deviation metrics Δ of NSGA-II algorithm and I-NSGA-II algorithm.

Numbers of running	Deviation measure Δ	
	NSGA-II	I-NSGA-II
1	25.7858	18.2390
2	25.0622	17.9382
3	27.1682	18.0339
4	26.0873	17.8360
5	25.0980	18.2301
6	25.6266	18.1926
7	24.5479	17.4007
8	24.7549	17.3698
9	25.3454	17.6387
10	24.6672	17.9725
Variance	0.63162	0.09347

6. Conclusion

In this paper, through analyzing the characteristics of the oil–gas production process, a multi-objective optimization model is established to maximize overall oil production of the block, minimize overall water production and comprehensive energy consumption for per ton oil, and NSGA-II algorithm is used to solve the proposed optimization model. In order to further improve the diversity and convergence of Pareto optimal solutions obtained by NSGA-II algorithm, an improved NSGA-II (I-NSGA-II) algorithm is proposed. The algorithm is based on NSGA-II algorithm, a new hybrid chaotic mapping model is first established to initialize population for keeping the initial population diversity. Then, the hybrid operator is composed to produce new generation of population for improving the search capability of NSGA-II algorithm. Finally, substitution operation of chaotic population candidate is introduced for maintaining the diversity and uniformity of obtained Pareto optimal solution set. The advantages of the proposed algorithm were demonstrated on several standard test problems and the actual production process of an oil recovery operation area studies. The results show that the Pareto optimal solution set obtained by I-NSGA-II algorithm has a better diversity, uniformity and convergence. Thus, the proposed optimization method provides a more reliable tool for the implementation of optimization control in oil production process, and it has a very important significance for the development of oil industry.

Acknowledgments

The authors would like to thank the editor and the reviewers for their helpful comments and high-quality suggestions. This work was supported by the Key Project of the National Natural Science Foundation of China (61034005), we also thank for the support from the Liaohe Oilfield of China, providing us research and experimental conditions.

References

[1] Rabiei M, Gupta R, Yaw Peng Cheong, Soto GAS. Excess water production diagnosis in oil fields using ensemble classifiers. In: International Conference on Computational Intelligence and Software Engineering; 2009. p. 1–4.
[2] Kosmidis VD, Perkins JD, Pistikopoulos EN. A mixed integer optimization formulation for the well scheduling problem on petroleum fields. Comput Chem Eng 2005;29:1523–41.
[3] Camponogara E, Plucenio A, Teixeira AF, Campos SRV. An automation system for gas-lifted oil wells: model identification, control, and optimization. J Petrol Sci Eng 2010;70:157–67.

[4] Zheng HJ, Deng JB. Research and application on designing method of sucker-rod pumping system with the least energy consumption. Acta Petrolei Sinica 2007;28:129–32.
[5] Dong SM, Li HQ, Yan XM, Zhang SL. Simulating maximum of system efficiency of rod pumping wells. J Syst Simul 2008;20:3533–7.
[6] Wu XD, Wu YQ, Han GQ, An YS, Wang YN. A new leakage model for rod pump. Acta Petrolei Sinica 2013;34:989–94.
[7] Dong SM, Zhang XS, Wu CJ, Guo JM. Simulation and optimization method for the integral energy-saving suction parameters of rod pumping wells in an oil field. Acta Petrolei Sinica 2010;31:475–9.
[8] Lang J, Tang LX. Modeling and Lagrangian relaxation based heuristic for scheduling oil wells in oilfield production. In: Proceedings of the 32nd Chinese Control Conference; 2013. p. 2554–9.
[9] Liu Y, Zhao HJ, Wang P. An optimizing design and analysis of oil gas gathering of ring type mixing hot water. Acta Petrolei Sinica 1999;20:77–81.
[10] He YF, Wang ZZ, Zhao YZ. Oil-gas gathering and transportation parameter optimization for electrical heating about ramiform net with single pipe. J Daqing Petrol Inst 2009;33:73–4.
[11] Wu YG. A study on optimal operation and energy saving of super heavy oil pipeline. In: 2011 International Conference on Computer Distributed Control and Intelligent Environmental Monitoring (CDCIEM); 2011. p. 400–3.
[12] Abbasi E, Garousi V. An MILP-based formulation for minimizing pumping energy costs of oil pipelines: Beneficial to both the environment and pipeline companies. Energy Syst 2010;1:393–416.
[13] Mahmoudimehr J, Sanaye S. Minimization of fuel consumption of natural gas compressor stations with similar and dissimilar turbo-compressor units. J Energy Eng 2014;140:1–9.
[14] Borraz-Sánchez C, Haugland D. Optimization methods for pipeline transportation of natural gas with variable specific gravity and compressibility. TOP 2013;21:524–41.
[15] Noori-Darvish S, Tavakkoli-Moghaddam R. Minimizing the total tardiness and make span in an open shop scheduling problem with sequence-dependent setup times. J Ind Eng Int 2012;8:1–13.
[16] Codas A, Campos S, Camponogara E, Gunnerud V, Sunjerga S. Integrated production optimization of oil fields with pressure and routing constraints: the Urucu field. Comput Chem Eng 2012;46:178–89.
[17] Kim MJ, Yoo CK. Multi-objective controller for enhancing nutrient removal and biogas production in wastewater treatment plants. J Taiwan Inst Chem Eng 2014;45:2537–48.
[18] Deb K, Pratap A, Agarwal S, Meyarivan T. A fast and elitist multi objective genetic algorithm: NSGA_II. IEEE Trans Evol Comput 2002;6:182–97.
[19] Maghouli P, Hosseini SH, Buygi MO, Shahidehpour M. A scenario-based multi-objective model for multi-stage transmission expansion planning. IEEE Trans Power Syst 2011;26:470–8.
[20] Senthilkumar C, Ganesan G, Karthikeyan R. Parametric optimization of electrochemical machining of Al/15% SiCp composites using NSGA-II. Trans Nonferrous Met Soc Chin 2011;21:2294–300.
[21] Jemai J, Zekri M, Mellouli K. An NSGA-II algorithm for the green vehicle routing problem. Lect Note Comput Sci 2012;7245:37–48.
[22] Panda S, Yegireddy NK. Automatic generation control of multi-area power system using multi-objective non-dominated sorting genetic algorithm-II. Int J Electrical Power Energy Syst 2013;53:54–63.
[23] Bensmaine A, Dahane M, Benyoucef Y. A non-dominated sorting genetic algorithm based approach for optimal machines selection in reconfigurable manufacturing environment. Comput Ind Eng 2013;66:519–24.
[24] Bayat M, Dehghani Z, Rahimpour MR. Dynamic multi-objective optimization of industrial radial-flow fixed-bed reactor of heavy paraffin dehydrogenation in LAB plant using NSGA-II method. J Taiwan Inst Chem Eng 2014;45:1474–84.
[25] Zhang GJ, Zhang Z, Ming WY, Guo JW, Huang Y, Shao XY. The multi-objective optimization of medium-speed WEDM process parameters for machining SKD11 steel by the hybrid method of RSM and NSGA-II. Int J Adv Manufact Technol 2014;70:2097–109.
[26] Pasandideh SHR, Niaki STA, Asadi K. Bi-objective optimization of a multi-product multi-period three-echelon supply chain problem under uncertain environments: NSGA-II and NRGA. Inf Sci 2015;292:57–74.
[27] Deb K, Agrawal S, Pratap A, Meyarivan T. A fast elitist non-dominated sorting genetic algorithm for multi-objective optimization: NSGA_II. In: 6th International Conference on Parallel Problem Solving From Nature; 2000. p. 849–58.
[28] Srinivas N, Deb K. Multi-objective optimization using non-dominated sorting in genetic algorithms. J Evol Comput 1994;2:221–48.
[29] Nojima Y, Narukawa K, Kaige S, Ishibuchi H. Effects of removing overlapping solutions on the performance of the NSGA-II algorithm. In: 3rd International Conference on Evolutionary Multi-Criterion Optimization; 2005. p. 341–54.
[30] Shukla PK. On gradient based local search in unconstrained evolutionary multi-objective optimization. In: Proceedings of the 4th International Conference on Evolutionary Multi-objective Optimization; 2007. p. 96–110.
[31] Brown M, Smith RE. Directed multi-objective optimization. Int J Comput 2005;6:3–17.
[32] Bęben A, Batalla JM, Chai WK, Śliwiński J. Multi-criteria decision algorithms for efficient content delivery in content networks. Ann Telecommun-Annales Des Télécommunications 2013;68:153–65.
[33] Zitzler E, Thiele L, Laumanns M, Fonseca CM, Fonseca VGD. Performance assessment of multi-objective optimizers: An analysis and review. IEEE Trans Evol Comput 2003;7:117–32.
[34] Usychenko VG. Tent map as an abstract model of open system evolution. Tech Phys 2011;56:885–8.
[35] Kong WJ, Ding JL, Chai TY, Sun J. Large-dimensional multi-objective evolutionary algorithms based on improved average ranking. In: 49th IEEE Conference on Decision and Control. Hilton Atlanta Hotel; 2010. p. 502–7.
[36] Yu G, Chai TY. Multi-objective production planning optimization using hybrid evolutionary algorithms for mineral processing. IEEE Trans Evol Comput 2011;15:487–513.
[37] Zitzler E, Thiele L. Multi-objective evolutionary algorithms: a comparative case study and the strength Pareto approach. IEEE Trans Evol Comput 1999;3:257–71.
[38] Zitzler E, Deb K, Thiele L. Comparison of multi-objective evolutionary algorithms: Empirical results. Evol Comput 2000;8:173–95.
[39] Niu DP, Wang FL, He DK, Jia MX. Chaotic differential evolution for multiobjective optimization. Control Decision 2009;24:361–4.

Please cite this article as: T. Liu et al., Multi-objective optimization method using an improved NSGA-II algorithm for oil-gas production process, Journal of the Taiwan Institute of Chemical Engineers (2015), http://dx.doi.org/10.1016/j.jtice.2015.05.026